

# Surface modification of Ni (50.6 at.%) Ti by high current pulsed electron beam treatment

K.M. Zhang<sup>a,1</sup>, J.X. Zou<sup>a,b,2</sup>, T. Grosdidier<sup>b,\*</sup>, N. Gey<sup>b,2</sup>,  
D.Z. Yang<sup>a,1</sup>, S.Z. Hao<sup>a,3</sup>, C. Dong<sup>a,4</sup>

<sup>a</sup> School of Materials Science and Engineering, State Key Laboratory of Materials Modification by Laser, Ion and Electron Beams, Dalian University of Technology, Dalian 116024, PR China

<sup>b</sup> Laboratoire d'Etude des Textures et Applications aux Matériaux (LETAM, UMR-CNRS 7078), Université Paul Verlaine Metz, Ile du Saulcy, 57012 Metz, France

Available online 10 October 2006

## Abstract

A Ni (50.6 at.%) Ti shape memory alloy having a grain size of 30–50  $\mu\text{m}$ , was subjected to high current pulsed electron beam (HCPEB) irradiation and the microstructure modifications were investigated in detail. The treatment induces superfaster melting and solidification at the top surface. As a result, the top surface melted layer solidified into a 600 nm fine grain austenite (B2) structure. A martensitic phase transformation occurred in the subsurface zone due to the high thermal stress induced by the HCPEB treatment. This transformation was avoided in the top surface melted layer. © 2006 Elsevier B.V. All rights reserved.

**Keywords:** Nanostructured materials; Thin films; Rapid solidification; Electron beam processing; Phase transitions

## 1. Introduction

NiTi alloys are widely used in the industrial fields due to their shape memory, super-elasticity effects and good corrosion resistance [1–3]. Previous studies have shown that the grain refinement of NiTi alloys can change the martensitic transformation temperature and lead to the extension of the shape recovery [4]. Also, the nature of the material surface is of major importance; in particular for corrosion and wear resistance properties. Therefore, surface treatment can be used to improve the material performance.

The interaction of high current pulsed electron beam (HCPEB) with materials has recently received enormous attention for surface treatment [5–12]. The HCPEB irradiation

induces dynamic temperature fields in the surface of the material, giving rise to superfaster heating and melting, as well as a dynamic stress field that causes intense deformation at the material surface. The combination of these processes makes it possible to modify substantially the surface characteristics and, in many cases, improve the mechanical properties faster and more efficiently than conventional surface treatment techniques.

In the present study, we will report, for the first time, the surface treatment of a NiTi shape memory alloy by the HCPEB technique.

## 2. Experimental procedures

### 2.1. Experimental equipments

The pulsed electron beam treatment was done using a Nadezhda-2 type HCPEB source. It produces an electron beam of low-energy (10–40 keV), high peak current ( $10^2$ – $10^3$  A/cm<sup>2</sup>), short pulse duration (approx. 1  $\mu\text{s}$ ) and high efficiency (repeating pulse interval being 10 s). More details about the principle of the HCPEB system are in references [9,11].

### 2.2. Starting material and samples preparation

The as-received Ni (50.6 at.%)Ti shape memory alloy was hot rolled at 750 °C in the form of a nearly rounded bar having a diameter of 12 mm. The initial grain size was about 30–50  $\mu\text{m}$ . The specimens for HCPEB treatment were

\* Corresponding author. Tel.: +33 387317130; fax: +33 387315377.  
E-mail addresses: zhangkemin2000@163.com (K.M. Zhang),  
jianxin.zou@univ-metz.fr (J.X. Zou), thierry.grosdidier@univ-metz.fr  
(T. Grosdidier), nathalie.gey@univ-metz.fr (N. Gey), dzyang@dlut.edu.cn  
(D.Z. Yang), shengzhi\_hao@yahoo.com.cn (S.Z. Hao), dong@dlut.edu.cn  
(C. Dong).

<sup>1</sup> Tel.: +86 411 84708441.

<sup>2</sup> Tel.: +33 387317130; fax: +33 387315377.

<sup>3</sup> Tel.: +86 411 84708380; fax: +86 411 84708389.

<sup>4</sup> Tel.: +86 411 84707930; fax: +86 411 84708389.

cut into 2 mm-thick discs and their surface was polished down to diamond paste. The electron beam treatment parameters were as follows: the accelerating voltage 27 kV and the energy density  $3 \text{ J/cm}^2$ . The samples investigated here were treated for five pulses with a pulse duration of  $1.5 \mu\text{s}$ . The dwell time between each pulse was 10 s.

### 2.3. Surface characterization

X-ray diffraction (XRD) analyses were carried out using a XRD-6000 goniometer from SHIMADZU, operating with the Cu  $K\alpha$  radiation. A JEOL 6500F type field emission gun scanning electron microscope (FEG-SEM) equipped with an electron backscattered diffraction (EBSD) attachment was used to observe surface morphologies and gain more information about the microstructure and texture states of the melted zone. The SEM was operating at 15 kV with the sample tilted by  $70^\circ$ . NiTi martensite (B19') and austenite (B2) were used for possible indexing during the EBSD analysis. The EBSD maps were acquired with a step size of 70 nm.

## 3. Results

### 3.1. Structure modification and phase transformation

Fig. 1 shows a typical optical micrograph of the treated sample surface. It shows two distinct features. The first one is the formation of craters, which is a typical feature of many HCPEB treated metal surfaces [9]. It has been observed that the precipitates were often located in the center of the craters [12]. It was established that the presence of interfaces or second phase affects the number of eruption events and the crater density. In particular, as the inclusions' physical properties such as density, heat conductivity, heat capacity and melting point are usually different from those of the matrix phase, they can act as nucleation sites. In the case of this alloy,  $\text{Ti}_2\text{Ni}$  are the initiation sites for craters. It was also observed that part of the  $\text{Ti}_2\text{Ni}$  precipitates which are not involved in the crater formation dissolve during melting. In consequence, the eruption phenomenon together with the dissolution of  $\text{Ti}_2\text{Ni}$  during the treatment, leads to the reduction of the precipitate density in the surface melted layer as well as a purification of this melted layer [12]. The second feature is the presence of many straight bands. Such kind of feature on a shape memory alloy can be associated with the martensitic transformation. The occurrence of the martensitic transformation after the HCPEB treatment was confirmed by

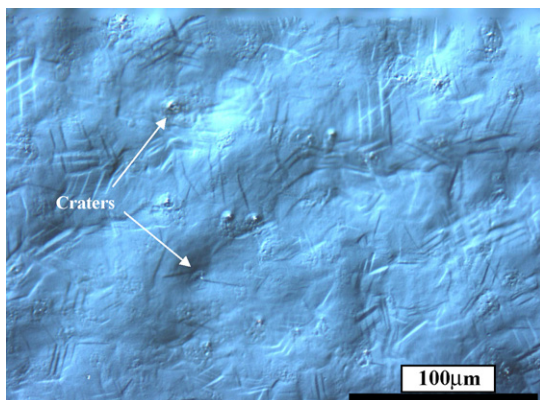


Fig. 1. Typical optical micrograph of the treated sample, showing craters and some phase transformation features remained on the top surface.

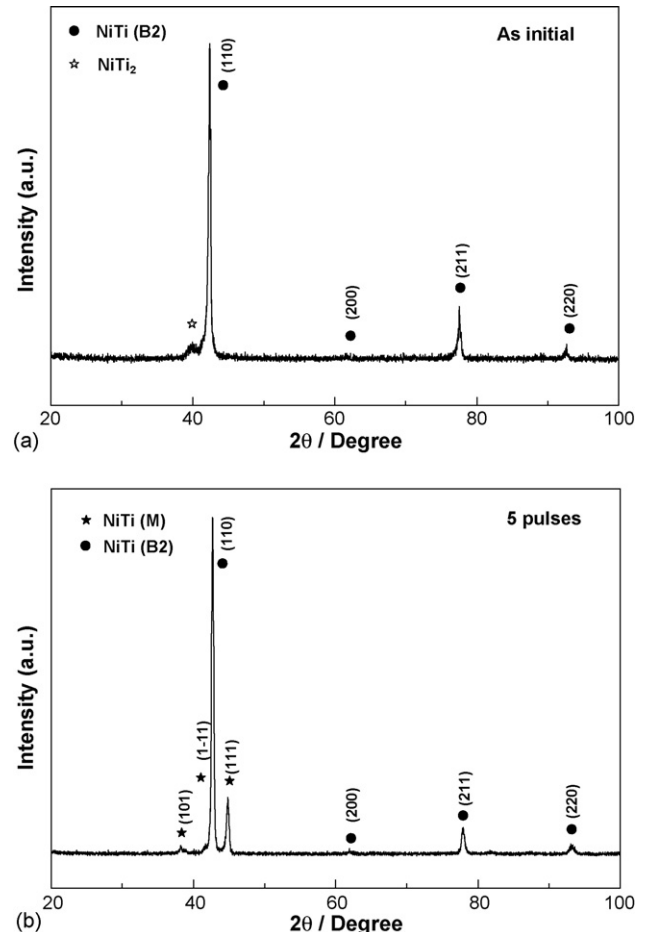


Fig. 2. XRD analysis of the untreated (a) and the treated sample (b), showing martensitic transformation occurred after HCPEB treatment.

XRD analysis carried out before and after treatments. Examples of diffractograms are shown in Fig. 2. For the initial state, the observed peaks correspond to the NiTi (B2 structure) austenite phase and the  $\text{Ti}_2\text{Ni}$  precipitates. After the HCPEB treatments, peaks corresponding to the NiTi martensitic phase (B19') [2] are present. It is also visible that the diffraction peaks of the  $\text{Ti}_2\text{Ni}$  have vanished: a direct consequence of the surface purification in the melted layer.

### 3.2. Grain refinement

To gain more information about the microstructure and texture issued from the solidification of the surface melted zone, FEG-SEM and EBSD were carried out to characterize the top surface of the treated sample. Fig. 3 shows a typical SEM morphology of the treated sample. Some bands can be clearly observed. In addition, there are many voids on the surface. The voids are shrinkage cavities resulting from the solidification process. Fig. 4 is a Kikuchi pattern quality (KPQ) map [13] taken from the same area. After the HCPEB treatment, the rapid solidification leads to a fine grain structure. The mean grain size was determined to be about 600 nm. All the grains on the top surface were indexed as corresponding to the NiTi austenitic phase having the B2 structure and no martensitic phase could be indexed.

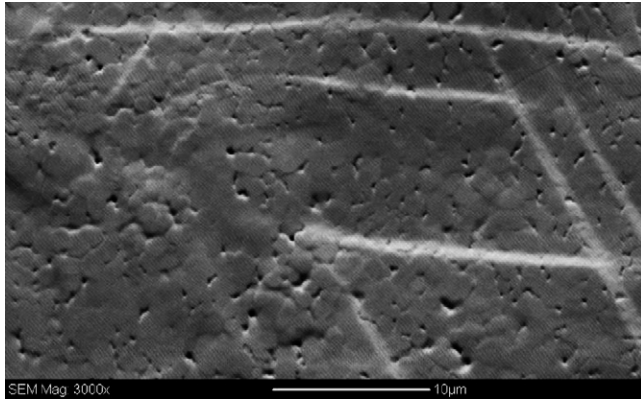


Fig. 3. Typical SEM morphology of the treated sample surface.

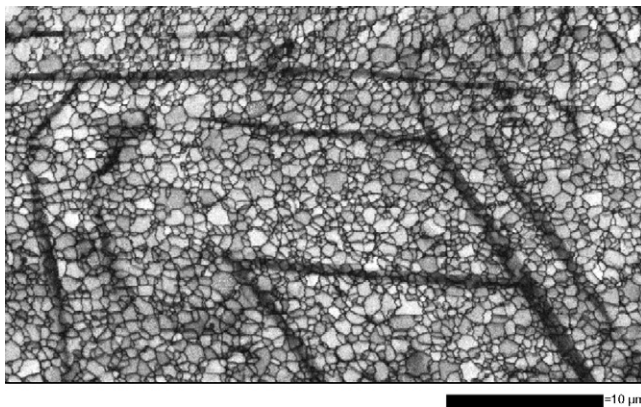


Fig. 4. EBSD KPM map taken from the same area as Fig. 3, showing very fine NiTi austenite (B2) grains formed after HCPEB treatment.

This indicates that the martensite revealed in the XRD trace in Fig. 2b is located at the subsurface, below the melted layer. It should be noted here that the dark areas in the KPM map correspond to the areas having a low quality of Kikuchi patterns. These band like areas could therefore correspond to areas where the B2 grains were constrained by the martensitic transformation occurring in the subsurface layer.

#### 4. Discussion

During the HCPEB bombardment, the concentrated energy flux acting on the NiTi alloy induces dynamic temperature fields in the surface layers where the energy has been deposited. This gives rise to superfast heating and melting followed by superfast solidification in the top surface melted zone of the material. The rapid solidification process occurred at rates as high as  $10^8$  K/s and led, in this alloy, to the formation of ultrafine B2 grains at the top surface. At the same time, a quasi-static thermal stress with an amplitude of several hundred MPa forms and causes intense deformations in the material [14]. For this NiTi alloy, the martensitic transformation temperature ( $M_s$ ) was measured for the untreated material to be about  $-1.5^\circ\text{C}$ , lower than the room temperature. Therefore, there was no martensite in the initial sample. For the treated sample, a stress induced martensitic transformation took place in the heat affected zone. This

martensitic transformation is triggered by the high quasi-static thermal stress produced by the HCPEB treatment. Interestingly, the martensitic transformation was not triggered in the melted zone. The fact that XRD could however very clearly depict the signal of the martensite suggest that the thickness of the melted layer is in the range  $2\text{--}3\ \mu\text{m}$ . It could be considered that the subsurface layer had significantly deformed while the melted zone was not yet solidified; thereby avoiding the effect of the shock wave. Alternatively, the fact that the indexing of the Kikuchi patterns from the ultrafine grains was very difficult along bands suggests that the grains located along these bands were already solidified and subsequently constrained by the martensitic transformation occurring in the subsurface layer. Several reasons can be called upon for this. Firstly, the eruption and dissolution of the  $\text{Ti}_2\text{Ni}$  precipitates in the melted zone result in a chemical change in this layer, which will influence the martensitic transformation temperature. Secondly, the melted layer contains very fine grains. Previous works have shown that the martensitic transformation temperature can be significantly decreased if the austenite grain is sufficient small [15,16]. Finally, the stress level may also be significantly different in the heat affected zone and in the melted layer. Further work is now under way to fully elucidate the formation mechanisms of the metastable structures formed under the action of this new promising surface treatment process.

#### 5. Summary and conclusion

This work has examined the effect of a new electron beam (HCPEB) treatment for modifying the surface of a shape memory Ni (50.6%)Ti alloy. A thin surface layer was melted by the action of the electron beam. This melted layer solidified as a very fine grain austenitic (B2) structure. A stress induced martensitic transformation was triggered after the HCPEB treatment in the subsurface material but was avoided in the fine grain structure of the thin melted layer. The formation mechanisms of these structures are the consequence of the rapid solidification in the surface melted layer and the result of the stresses associated with the propagation of the shock wave in the subsurface layer.

#### References

- [1] C.M. Jackson, R.J. Wagner, R.J. Wasilewski, NiTi Shape Memory Alloys, NASA Report No. NASA-SR-5110, 1972.
- [2] X. Xu, N. Thadhani, Mater. Sci. Eng. A 384 (2004) 194–201.
- [3] H.C. Man, Z.D. Cui, T.M. Yue, Scr. Mater. 45 (2001) 1447–1453.
- [4] F.X. Gil-Mur, D. Rodriguez, J.A. Planell, Proceedings of the Titanium '95: Sci. Technol., 1995, pp. 2399–2406.
- [5] J. Gyulai, I. Krafscic, Nucl. Instrum. Meth. B 37/38 (1989) 275–287.
- [6] Y. Nakagawa, T. Arioshi, M. Itamy, Y. Fujii, Jpn. J. Phys. 27 (1988) L719.
- [7] A. Zecca, R.S. Brusa, M. Duarte, J. Paridaence, A.D. Pogrebnyak, A.B. Markov, G.E. Ozur, D.I. Proskurovskii, V.P. Rotstein, Phys. Lett. 175 (1993) 433–437.
- [8] D.I. Proskurovsky, V. Rotshtein, G.E. Ozur, Surf. Coat. Technol. 96 (1) (1997) 115–122.
- [9] D.I. Proskurovsky, V. Rotshtein, G.E. Ozur, A.B. Markov, D.S. Nazarov, J. Vac. Sci. Technol. A 1694 (1998) 2480–2488.
- [10] A.D. Pogrebnyak, S. Bratushka, V.I. Boyko, I.V. Shamanin, Y.V. Tsvintarnaya, Nucl. Instrum. Meth. Phys. Res. B 145 (1998) 373–390.

- [11] C. Dong, A. Wu, S. Hao, J. Zou, Z. Liu, P. Zhong, A. Zhang, T. Xu, J. Chen, J. Xu, Q. Liu, Z. Zhou, *Surf. Coat. Technol.* 163/164 (2003) 620–624.
- [12] J.X. Zou, K.M. Zhang, C. Dong, Y. Qin, S.Z. Hao, T. Grosdidier, *Appl. Phys. Lett.* 89 (2006) 041913.
- [13] F.J. Humphreys, *Scrip. Mater.* 51 (2004) 771–776.
- [14] Y. Qin, J.X. Zou, C. Dong, X.G. Wang, A.M. Wu, Y. Liu, S.Z. Hao, Q.F. Guan, *Nucl. Instrum. Meth. Phys. Res. B* 225 (2004) 544–554.
- [15] Q.P. Meng, Y.H. Rong, T.Y. Hsu, *Phys. Rev. B* 65 (2002) 174118-1-7.
- [16] G.N. Haidemenopoulos, M. Grujicic, G.B. Olson, M. Cohen, *J. Alloys Compd.* 220 (1995) 142–147.